Research Article | Vol. 25, No. 26 | 25 Dec 2017 | OPTICS EXPRESS 32879
Optics EXPRESS

Femtosecond inscription and thermal testing of Bragg gratings in high concentration (40 mol%) germania-doped optical fibre

A. Donko,* M. Nuñez-Velazquez, P. Barua, F. Guzman Cruz, R. Ismaeel, T. Lee, J. K. Sahu, M. Beresna, and G. Brambilla

Optoelectronics Research Centre, University of Southampton, Southampton, SO17 1BJ, UK
**a.l.donko@soton.ac.uk*

Abstract: Using point-by-point infrared femtosecond laser inscription, a fibre Bragg grating with a resonance wavelength of 1550.28±0.02 nm, 25 dB extinction ratio, and 1.10±0.02 nm bandwidth (measured at first minima) was inscribed in a high concentration (40 mol%) germania-doped silica fibre. At this wavelength, the high concentration germania doped silica fibre had a normalized frequency of V ≃ 3.06 permitting higher order mode propagation. Subsequently, two additional Bragg resonances were recorded at 1534.40 ± 0.02 and 1535.78 ± 0.02 nm, corresponding to the coupling of the forward propagating fundamental mode and counter propagating HE_{21} and TM_{01}/TE_{01}, respectively. Thermal tests revealed the grating was stable up to 800 °C for 30 minutes. Analysis determined the grating had first and second order coefficients $d\lambda_B/dT$ = 11.1 pm/°C and $d^2\lambda_B/dT^2 = 8.37 \times 10^{-3}$ pm^2/°C^2 respectively.

OCIS codes: (060.3735) Fiber Bragg gratings; (320.2250) Femtosecond phenomena.

References and links

1. F. L. Galeener, J. C. Mikkelsen, R. H. Geils, and W. J. Mosby, "The relative Raman cross sections of vitreous SiO2, GeO 2, B2O3, and P2O5," Appl. Phys. Lett. **32**, 34–36 (1978).
2. A. Boskovic, S. V. Chernikov, J. R. Taylor, L. Gruner-Nielsen, and O. A. Levring, "Direct continuous-wave measurement of n_2 in various types of telecommunication fiber at 1.55 microm," Opt. Lett. **21**(24), 1966–1968 (1996).
3. H. S. Seo, K. Oh, and U. C. Paek, "Gain optimization of germanosilicate fiber raman amplifier and its applications in the compensation of raman-induced crosstalk among wavelength division multiplexing channels," IEEE J. Quantum Electron. **37**, 1110–1116 (2001).
4. E. M. Dianov and V. M. Mashinsky, "Germania-Based Core Optical Fibers," J. Lightwave Tech. **23**, 3500–3508 (2005).
5. V. M. Mashinsky, V. B. Neustruev, V. V. Dvoyrin, S. A. Vasiliev, O. I. Medvedkov, I. A. Bufetov, A. V. Shubin, E. M. Dianov, A. N. Guryanov, V. F. Khopin, and M. Y. Salgansky, "Germania-glass-core silica-glass-cladding modified chemical-vapor deposition optical fibers: optical losses, photorefractivity, and Raman amplification," Opt. Lett. **29**(22), 2596–2598 (2004).
6. B. Malo, K. O. Hill, F. Bilodeau, D. C. Johnson, and J. Albert, "Point-by-point fabrication of micro-Bragg gratings in photosensitive fibre using single excimer pulse refractive index modification techniques," Electron. Lett. **29**, 1668 (1993).
7. K. O. Hill, Y. Fujii, D. C. Johnson, and B. S. Kawasaki, "Photosensitivity in optical fiber waveguides: Application to reflection filter fabrication," Appl. Phys. Lett. **32**, 647–649 (1978).
8. G. Meltz, W. W. Morey, and W. H. Glenn, "Formation of Bragg gratings in optical fibers by a transverse holographic method," Opt. Lett. **14**(15), 823–825 (1989).
9. R. Kashyap, A. Swanton, and R. Smith, "Infinite length fibre gratings," Electron. Lett. **35**, 1871–1872 (1999).
10. M. Lancry and B. Poumellec, "UV laser processing and multiphoton absorption processes in optical telecommunication fiber materials," Phys. Rep. **523**, 207–229 (2013).
11. J. Canning, "Photosensitization and Photostabilization of Laser-Induced Index Changes in Optical Fibers," Opt. Fiber Technol. **6**, 275–289 (2000).
12. L. Dong, J. Pinkstone, P. S. J. Russell, and D. N. Payne, "Ultraviolet absorption in modified chemical vapor deposition preforms," JOSA B **11**, 2106–2111 (1994).
13. O. I. Medvedkov, S. A. Vasiliev, P. I. Gnusin, and E. M. Dianov, "Photosensitivity of optical fibers with extremely high germanium concentration," Opt. Mater. Express **2**, 1478 (2012).

#304867 https://doi.org/10.1364/OE.25.032879
Journal © 2017 Received 17 Aug 2017; revised 20 Oct 2017; accepted 5 Nov 2017; published 18 Dec 2017

Optics EXPRESS

14. K. M. Davis, K. Miura, N. Sugimoto, and K. Hirao, "Writing waveguides in glass with a femtosecond laser," Opt. Lett. **21**(21), 1729–1731 (1996).
15. H. G. Limberger, C. Ban, R. P. Salathé, S. A. Slattery, and D. N. Nikogosyan, "Absence of UV-induced stress in Bragg gratings recorded by high-intensity 264 nm laser pulses in a hydrogenated standard telecom fiber," Opt. Express **15**(9), 5610–5615 (2007).
16. J. W. Chan, T. Huser, S. Risbud, and D. M. Krol, "Structural changes in fused silica after exposure to focused femtosecond laser pulses," Opt. Lett. **26**(21), 1726–1728 (2001).
17. A. Martinez, M. Dubov, I. Khrushchev, and I. Bennion, "Direct writing of fibre Bragg gratings by femtosecond laser," Electron. Lett. **40**, 1170 (2004).
18. M. Ams, G. Marshall, D. Spence, and M. Withford, "Slit beam shaping method for femtosecond laser direct-write fabrication of symmetric waveguides in bulk glasses," Opt. Express **13**(15), 5676–5681 (2005).
19. T. Mizunami, T. V. Djambova, T. Niiho, and S. Gupta, "Bragg gratings in multimode and few-mode optical fibers," J. Lightwave Technol. **18**, 230–235 (2000).
20. Y.-G. Han, S. B. Lee, D. S. Moon, and Y. Chung, "Investigation of a multiwavelength raman fiber laser based on few-mode fiber Bragg gratings," Opt. Lett. **30**(17), 2200–2202 (2005).
21. K. Okamoto, "Optical Fibres," in *Fundamentals of Optical Waveguides* (Elsevier, 2006), Chap. 3.
22. W. J. Tropf, M. E. Thomas, and T. J. Harris, *Handbook Of Optics* (Elsevier, 1995), Chap. 33.
23. Y. Li, C. R. Liao, D. N. Wang, T. Sun, and K. T. V. Grattan, "Study of spectral and annealing properties of fiber Bragg gratings written in H2-free and H2- loaded fibers by use of femtosecond laser pulses," Opt. Express **16**(26), 21239–21247 (2008).
24. B. H. Kim, Y. Park, T. J. Ahn, D. Y. Kim, B. H. Lee, Y. Chung, U. C. Paek, and W. T. Han, "Residual stress relaxation in the core of optical fiber by CO2 laser irradiation," Opt. Lett. **26**(21), 1657–1659 (2001).
25. G. Meltz and W. W. Morey, "Bragg grating formation and germanosilicate fiber photosensitivity," in *International Workshop on Photoinduced Seff-Organization Effects in Ontical Fibe* (1991).
26. A. Donko, M. Nunez-Velazquez, and M. Beresna, "Femtosecond Inscription And Thermal Testing Of Bragg Gratings In High Concentration Germania-Doped Optical Fibre," Figshare 2017 [retrieved 14 August 2017] *https://doi.org/10.5258/SOTON/D0215*.
27. E. F. Riebling, "Nonideal Mixing in Binary Ge0,-SiO, Glasses," J. Am. Ceram. Soc. **51**, 406–407 (1968).
28. J. Oishi and T. Kimura, "Thermal Expansion of Fused Quartz Thermal Expansion of Fused Quartz," Meterologia **5**, 50–55 (1969).
29. G. Adamovsky, S. F. Lyuksyutov, J. R. Mackey, B. M. Floyd, U. Abeywickrema, I. Fedin, and M. Rackaitis, "Peculiarities of thermo-optic coefficient under different temperature regimes in optical fibers containing fiber Bragg gratings," Opt. Commun. **285**, 766–773 (2012).

1. Introduction

High concentration germania-doped fibres are of great interest due to their relative transparency at longer wavelengths and their attractive non-linear properties. In fact, germania has the highest peak value of Raman scattering cross section amongst the main glass forming oxides – it is 9.2 times higher than in silica at a glass frequency shift of 420 cm^{-1} [1] – allowing for highly efficient germania doped Raman fibre lasers and amplifiers tuneable across a wide spectral range. Furthermore, the non-linear refractive index coefficient n_2 is 3 times greater than silica, which has been proven beneficial for four wave mixing frequency conversion [2]. Seo et. al observed these advantageous properties of germania, recording a doubling in the Raman gain coefficient when the normalised refractive index difference of the core and cladding Δn, was increased from 0.005 to 0.04 at a glass frequency shift of 440 cm^{-1} [3]. The attractive traits of germania have led to extensive research into pure germania fibres and their successful fabrication has been extensively reported [4,5].

Despite these properties, the exploitation of high concentration (40 mol%) germania-doped waveguides has been limited due to the difficulties encountered in the manufacture of fibre Bragg gratings (FBGs). Since Hill et al observed the grating formation within a germania-doped silica fibre, fabrication techniques relied on exploiting UV-photosensitive materials for the following three decades [6–9]. At low writing intensities (<GW/cm^2) the photosensitive phenomena can be explained through a process of material densification and a change in the defect population [10,11]. As the germania concentration is increased within the fibre core, the linear absorption at short wavelengths increases and the balance of the underlying physical processes evolves depending on the inscription intensity. It has been reported that at 242 nm the absorption coefficient of a germania doped silica fibre α_{242} scales with the concentration by 36 dB/mm per mole % of germania - for a 40 mol% germania-

Optics EXPRESS

doped silica fibre α_{242} = 1.44 dB/μm [12]. Due to this high absorption, FBG fabrication in high concentration germania fibres leads to the formation of asymmetric grating planes with poor phase coherence and cladding mode generation; in-turn, this leads to the fabrication of a poor spectral quality reflector. The complex dynamics of the phenomena has been well documented and makes inscription of good spectral quality FBGs in high concentration germania fibres an extremely difficult task [12,13].

The discovery of ultrashort pulse interactions within transparent bulk glass created a new fabrication mechanism of FBGs [14]. Multiphoton absorption and avalanche ionization are responsible for causing a strong refractive index change in amorphous silica, often larger than 10^{-3}. At low energies, the former process is understood to break Si-O bonds (colour centre formation), while the latter causes the melting and resolidification of the glass [15,16]. Micro-Raman spectroscopy has revealed an increase in concentration of 3 and 4 member rings during the resolidification causes densification of the laser focal volume. The contribution of a multiphoton absorption leads to seed electrons necessary for avalanche ionization and as a result, there is very little dependence of the threshold writing intensity for optical breakdown on the bandgap of the material. These mechanisms remove the photosensitive prerequisite for FBG fabrication and in 2004, Martinez et. al inscribed a first, second and third order gratings within a standard telecom fibre using an infrared femtosecond laser [17].

Thus, femtosecond laser writing bypasses the limitations of complex photosensitive profiles initially imposed by classical techniques and makes inscription in germania-doped fibres possible. In this letter, we report the first good spectral quality FBG inscribed within a high concentration (40%mol) germania-doped fibre using point-by-point femtosecond laser inscription. In addition, we report the results of the thermal stability testing performed after inscription.

2. Experimental methodology

The fibre was drawn from a preform manufactured in house using the modified chemical vapour deposition (MCVD). A high refractive index acrylate DSM-314 cured by photo-polymerisation coated the fibre to prevent cladding mode propagation. A multi-wavelength optical fibre analyser (IFA-100) was used to measure the fibre refractive index profile to a spatial resolution of 0.2 μm and accuracy of ± 1.0 × 10^{-4}. Figure 1 displays the refractive index profile of the fibre. The measurement found that the core and cladding had diameters of d_{co}~3.72 μm and d_{cl}~106 μm, respectively.

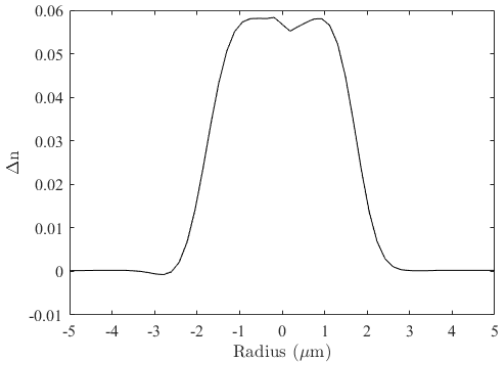

Fig. 1. Refractive index profile of the NA~0.41 germania-doped silica fibre showing a slight graded index distribution between cladding and core.

A standard point-by-point inscription set-up was assembled, a schematic of which can be seen in Fig. 2. A 1030 nm solid state Yb:KGW (ytterbium-doped potassium gadolinium tungstate) based femtosecond laser (PHAROS, Light Conversion Limited) was used for inscription and operated at a repetition rate of 1 kHz. Each pulse had a temporal duration of

Optics EXPRESS

206 ± 5 fs and a pulse energy of 1.1 ± 0.1 µJ. At the focal volume there was a peak intensity of 1.3 ± 0.1 TW/cm^2. A diffraction slit was placed prior to a 0.65 NA objective lens, while a dichroic mirror and digital camera were placed directly above the objective to enable monitoring of the writing process. The diffraction slit is a common alternative to other beam-shaping optics in femtosecond writing arrangements, serving the purpose of controlling the symmetry of the induced modification cross section [18]. In our case it allowed achieving better overlap of inscribed grating with the core of the fibre. The fibre was secured to a high precision (± 0.1 µm), computer controlled translation stage (Aerotech). Gratings were written by traversing the fibre beneath the objective and inscribing each refractive index modification individually. The FBG pitch was controlled by the synchronisation of fibre position with a pulse picker integrated within the femtosecond system using a controller (Aerotech). As an infrared inscription wavelength was used, the fibre coating did not require removal due to its relative transparency at this wavelength. The transmission spectra of the gratings were monitored in situ using a supercontinuum source (Fianium) and an optical spectrum analyser (OSA, Yokogawa).

After inscription, the grating's thermal stability was tested by removing the polymer coating and placing the grating within a 400 mm tubular furnace. Temperatures were validated by an external thermocouple. The fibre was thermally tested from room temperature to 800 °C. Transmission spectra were recorded at 50 °C increments from 50 °C. Transmission spectra of the grating were recorded after isochronal periods of 30 minutes using the supercontinuum source and OSA.

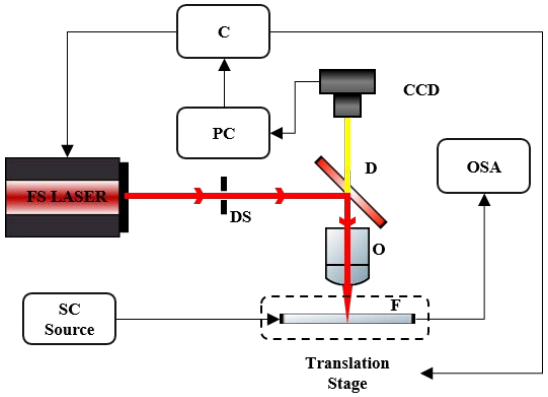

Fig. 2. Schematic of the femtosecond inscription set-up. **O**-Objective, **D**-dichroic mirror, **F**-fibre, **DS**-diffraction slit, (**C**)-synchronisation controller, **CCD**-CCD camera, **OSA**-optical spectrum analyser.

3. Results

3.1 FBG

A 3 mm 3rd order grating of 1.6 µm pitch was inscribed at a speed of 0.1 mm/s, with a design wavelength of 1550 nm. At 1550 nm, the normalized frequency of the fibre was calculated at $V \simeq 3.06$, implying four vectorial modes (HE_{11}, TE_{01}, TM_{01} and HE_{21}) are supported. The resultant transmission spectra is shown in Fig. 3(a). Three Bragg resonances are visible at λ_B = 1534.40 ± 0.02, 1535.78 ± 0.02 and 1550.28 ± 0.02 nm of extinction ratios 16, 5 and 25 dB, and bandwidths of 0.82 ± 0.02, 0.93 ± 0.02 and 1.10 ± 0.02 nm respectively. Bandwidths were measured at first minima. A computer program, based upon chi-squared analysis, ran an iterative algorithm to apply a line of best fit to the λ_B = 1550.28 ± 0.02 resonance and deduced a refractive index change of 6.4 ± 0.1 × 10^{-4}. The λ_B = 1550.28 ± 0.02 nm resonance corresponds to the self-coupling between the forward and counter propagating HE_{11} modes. The additional resonances at λ_B = 1534.40 ± 0.02 and 1535.78 ± 0.02 are attributable to the

Optics EXPRESS

fundamental mode coupling to higher order modes [19,20]. As only the fundamental mode was launched, no self-coupling between the forward and counter propagating higher order modes occurs. Backward propagating higher order modes were excited from the presence of the induced dielectric perturbation. Computational simulations (COMSOL Multiphysics) showed degeneracy of the TE_{01} and TM_{01} modes with an effective modal index of n_{eff} = 1.4583 (Table 1).

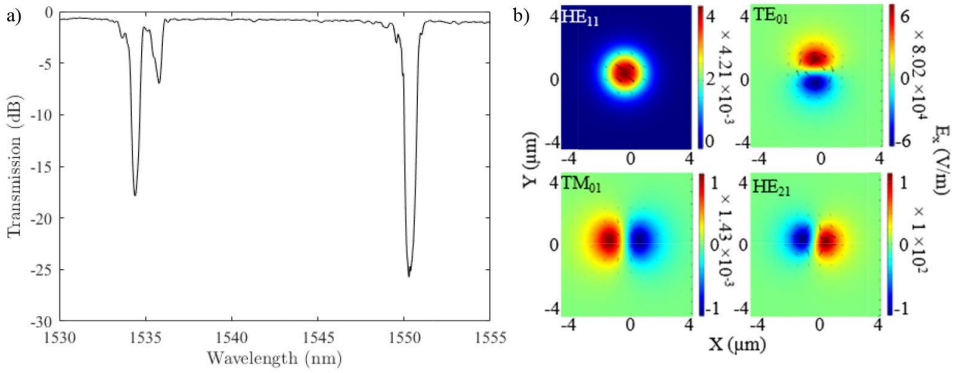

Fig. 3. (a) Transmission spectra of the FBG of resonance wavelength λ_B = 1550.28 nm. Additional resonances at λ_B = 1534.40 nm and λ_B = 1535.78 nm were also observed, attributable to the forward propagating HE_{11} mode coupling to the counter propagating higher order modes. (b) Simulated electric field (x component) of the HE_{11}, TE_{01}, TM_{01} and HE_{21} modes. The HE_{11} and HE_{21} had effective modal indices of $_{neff}$ = 1.4850 and n_{eff} = 1.4578, respectively. The TE_{01} and TM_{01} modes were degenerate with an effective modal index of n_{eff} = 1.4583.

In a standard step index fibre the degeneracy of these two modes is not physically permitted as the discontinuity between the refractive indices of the core and the cladding experienced by the electric field causes the TM_{01} mode to possess a lower effective modal index. As the TE_{01} electric field is orientated parallel to the boundary, no discontinuity is experienced - see Fig. 3(b) displaying the x-component electric field for the first four modes. Thus, the TE_{01} experiences a higher effective modal index. However, given the approximately graded refractive index profile of the germania-doped fibre, the TM_{01} electric field does not experience a discontinuity across the core - cladding boundary and hence propagates with the same effective modal index. The HE_{21} is not degenerate with the TM_{01} and TE_{01} as it is not radially similar; electric field lines from points on the cladding-air boundary tend back to a point on the cladding-air at an angle of 90 degrees bisecting the central fibre axis. Thus, as a higher percentage of power is carried within the cladding of the fibre the effective modal index of the HE_{21} mode is lower than that of the TM_{01} and TE_{01} [21].

Thus, the simulations inform us that the λ_B = 1534.40 nm resonance corresponds to the forward propagating HE11 mode coupling to the counter propagating TE_{01} and TM_{01} modes. Furthermore, the λ_B = 1535.78 nm resonance represents the coupling between the forward propagating fundamental mode and the counter propagating HE21 mode.

To compare the simulated and experimental results, the Bragg condition can be used to derive the following relationships between the recorded Bragg resonance wavelengths and theorised effective modal indices:

$$\frac{\lambda_x}{\lambda_y} = \frac{2n_{HE11}}{n_{HE11} + n_{TM01}} \quad (1)$$

Optics EXPRESS

$$\frac{\lambda_x}{\lambda_Z} = \frac{2n_{HE11}}{n_{HE11} + n_{HE21}} \tag{2}$$

where λ_x is the Bragg wavelength of the fundamental mode self coupling resonance; λ_y is the Bragg wavelength of the HE_{11} - TM_{01} / TE_{01} cross coupling resonance; λ_Z is the Bragg wavelength of the HE_{11} - HE_{21} cross coupling resonance; n_{HE11} is the effective modal index of the HE_{11} mode, n_{TM01} is the effective modal index of the TM_{01} / TE_{01} modes and n_{HE21} is the effective modal index of the HE_{21} mode. The results of these ratios were in agreement to ± 1% (Table 1).

Table 1. – Calculated effective modal indices and measured wavelengths of Bragg resonances. Below, a comparison of the simulated and theoretical results using Eq. (1) and (2). The simulated and theoretical results are in agreement to 1%.

Simulation		**Experiment**	
Mode	*Modal Index*	*Coupled Modes*	*Bragg resonance wavelength (nm)*
HE_{11}	1.4850	$HE_{11} - HE_{11}$	1550.28±0.02
TM_{01} / TE_{01}	1.4583	$HE_{11} - TE_{01}$ / TM_{01}	1535.78±0.02
HE_{21}	1.4578	$HE_{11} - HE_{21}$	1534.40±0.02
Ratio of effective indices		*Ratio of resonance wavelengths*	
$\frac{2n_{HE11}}{n_{HE11} + n_{TM01}}$	1.0091	$\frac{\lambda_x}{\lambda_y}$	1.0094
$\frac{2n_{HE11}}{n_{HE11} + n_{HE21}}$	1.0092	$\frac{\lambda_x}{\lambda_z}$	1.0103

3.2 Thermal testing

Frequently FBGs are thermally annealed to produce the most uniform refractive index modulations possible [22]. Similar to UV written gratings, it is likely the refractive index modifications are attributable to the highly non-linear defect formation resulting from the multi-photon absorption process [23]. Those defects can be annealed below the glass transition temperature in a similar manner to type I-UV gratings. On this basis, our fibre with inscribed FBG was annealed for 10 hours at 500 °C . The process was successful in removing thermal history; after the fibre cooled a non-reversible −3.28 ± 0.02 nm shift in the Bragg resonance wavelength was observed at 20 °C. This shift corresponds to a decrease of 3.1×10^{-6} in the effective index of the fundamental mode. The reduction observed is due to the release of stress induced from the drawing process during the fibre's fabrication [24].

The recorded transmission spectra can be seen in Fig. 4(a); only the fundamental resonance shift is displayed although uniform shifting of all grating spectra features was observed. The transmission spectra obtained showed a clear shift of the Bragg resonance to longer wavelengths as temperature was increased. Furthermore, as the temperature was increased to 800°C, the transmission at the Bragg wavelength varied between −23 to −29dB, which corresponds to linear reflectivity fluctuations of only < 1% from that at room temperature. These fluctuations can be attributed a low signal to noise ratio caused by inefficient coupling. In addition, the bandwidth of the self-coupling fundamental mode resonance remained constant at 1.10 ± 0.02 nm throughout the test. Due to the asymmetry of the Bragg resonance trough, the central wavelength was determined by the midpoint of the bandwidth at first minima.

Optics EXPRESS

Thermal tests revealed a reversible shift in the Bragg resonance wavelength with temperature. Figure 4(b) shows a plot of temperature against the central wavelength. A non-linear relationship was observed between temperature and wavelength. From 20 to 800 °C the first and second order coefficients were calculated from the regression line to be $d\lambda_B/dT$ = 11.1 pm/°C and $d^2\lambda_B/dT^2 = 8.37 \times 10^{-3}$ pm^2/°C^2, respectively. By taking small segments of temperature increases, the wavelength shift exhibits a linear increase. From 20 to 100 °C, the fibre had a linear sensitivity $d\lambda_B/dT$ = 12.10 ± 0.01 pm/°C. From 700 to 800 °C the fibre sensitivity increased $d\lambda_B/dT$ = 20.20 ± 0.01 pm/°C. Previously, non-linearity has been observed in a low concentration germania-doped silica fibre [25]. In comparison to the 9 mol% germania-doped silica fibre from 0 to 100 °C, the high concentration fibre is 35% more sensitive and from 700 to 800 °C it is 82% more sensitive.

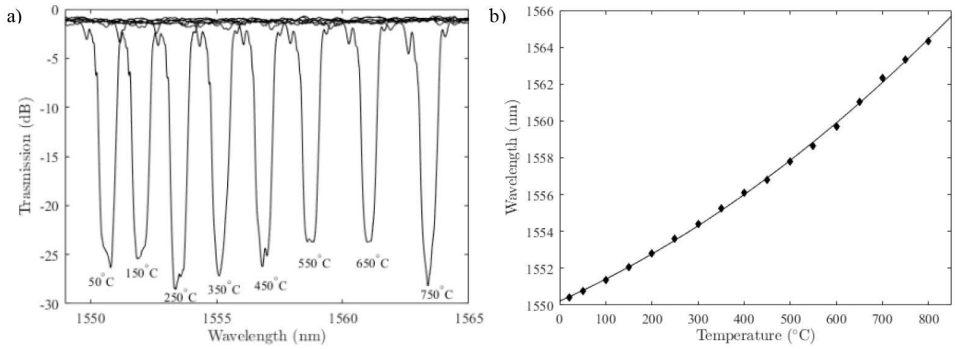

Fig. 4. (a) Transmission spectra of the FBG during thermal testing. The spectra only shows the shift of the fundamental Bragg resonance of λ_B = 1550.28 nm (at room temperature) from 50 to 750 °C. All other spectral features were observed to shift uniformly with the main Bragg resonance. (b) Thermal sensitivity plot of the high concentration germania fibre (solid). Regression analysis determined a quadratic correlation between the Bragg wavelength shift and temperature. Dataset 1 is available at [26].

The thermally dependent non-linear behavior is attributable to two material properties: the thermal expansion coefficient and the thermo-optic coefficient. Any drawing induced stresses from the photo-elastic effect were released during the annealing process. From literature, the germania-silica core has a thermal expansion coefficient almost a factor of 8 greater than that of the fused silica cladding ($\alpha_{core} = 43.7 \times 10^{-7}$ K^{-1} [27], $\alpha_{cladding} = 5.6 \times 10^{-7}$ K^{-1} [28].) The stark difference in the expansion rates causes a significant change in the stress field within the core. This relationship is linear in nature and thus it contributes solely to the linear coefficient measured. Secondly, the thermo-optic coefficient deriving from the polarizability of the material also varies with temperature. As temperature increases, atomic and lattice vibrations are generated, while thermal stimulation excites electrons to higher levels, raising the magnitude of the dipole moments [22]. The rate of change of the thermo-optic coefficient has been reported to fluctuate with increasing temperature in fused silica – a minimum is observed at 400 degrees [29]. Similar fluctuations were not observed in the 40 mol.% germania fibre. Only a continual increase in the rate of wavelength shift was observed. Reasons for this discrepancy are not clear and require further testing. Thus, given the linear contribution of the thermal expansion coefficient, the non-linear behaviour can be attributed to increases in the thermo-optic coefficient.

4. Conclusion

In conclusion, results of a good spectral quality Bragg grating inscribed in a 40 mol% germania-doped silica fibre have been presented. Thermal testing has revealed the fibre possesses a temperature sensitivity suitable for temperature sensing applications.

Optics EXPRESS

Furthermore, it has proven stable up to 800 °C with negligible (< 1%) effect on the grating reflectivity for 30 minutes. Thus, femtosecond laser writing has overcome issues faced by classical UV based techniques to inscribe Bragg gratings into 40 mol% germania-doped silica fibre and higher. By exploiting the negligible core material absorption in the near infrared wavelength range and relying on multiphoton absorption and avalanche ionisation, femtosecond fabrication of FBGs is not limited by the germania concentration; theoretically it is possible to write in 100% germania doped fibre. The results are a positive step towards making germania-doped Raman lasers and amplifiers a practical possibility. Further refinement to control the grating reflectivity will be required in order to form a cavity.

Funding

Engineering and Physical Sciences Research Council (EPSRC); Consejo Nacional de Ciencia y Tecnología.

Acknowledgements

The authors gratefully acknowledge the Engineering and Physical Sciences Research Council (EPSRC) for partially supporting the research project through grant. Andrei Donko would like to thank EPSRC for providing his studentship through the DTP. In addition, all authors would like to thank the additional support from The Royal Academy of Engineering and the Centre for Innovative Manufacturing in Photonics and CONACyT-Mexico.